Measurement 118 (2018) 298–310

Contents lists available at ScienceDirect

Measurement

journal homepage: www.elsevier.com/locate/measurement

Statistical analysis of colour changes in tempera paints mock-ups exposed to urban and marine environment

T. Rivas [a], J.S. Pozo-Antonio [a,*], D. Barral [a], J. Martínez [b], C. Cardell [c]

[a] Dept. de Enxeñaría dos Recursos Naturais e Medio Ambiente, Escola de Enxeñaría de Minas e Enerxía, Universidade de Vigo, 36310, Spain
[b] Dept. of Mathematics and Statistics, Centro Universitario de la Defensa, Escuela Naval Militar, Plaza de España, Marín 36920, Spain
[c] Dept. of Mineralogy and Petrology, University of Granada, Av. Fuentenueva s/n, Granada 18071, Spain

ARTICLE INFO

Article history:
Received 28 February 2017
Received in revised form 15 June 2017
Accepted 27 June 2017
Available online 28 June 2017

Keywords:
Tempera paint mock-ups
Egg yolk
Rabbit glue
Vectorial analysis
Functional analysis
Outdoor exposure

ABSTRACT

The aim of this study is the exploration of the suitability of two different statistical approaches (vectorial and functional analyses), which go beyond a purely descriptive statistics, in order to identify trends and similarities in colour changes of several tempera mock-ups paints during thirteen months. The samples were subjected under an outdoor exposure to a natural urban atmosphere characterized by an important marine and industrial influence. The changes of the colour were measured in CIE L*a*b* and CIE L*C*h colour spaces The paint mock-ups were binary mixtures made with either egg yolk or rabbit glue binder, mixed with one of the seven pigments studied, some of which have different grain sizes. Two different statistical analyses – vectorial and functional – were performed in order to detect the different colour change evolution among the temperas during the exposure time. The functional approach revealed more useful information than the vectorial (classic) one. Paints containing haematite, lapis lazuli and (standard grain size) azurite exhibited different trends of the colour parameters in comparison with the rest of the paints. Stereomicroscopy, X-ray diffraction and Fourier transform infrared spectroscopy showed that the binder composition and especially its stability to outdoor exposure, are the factors responsible for the statistically significant colour changes detected.

1. Introduction

Tempera painting is a technique where inorganic pigments are mixed with a protein binder such as rabbit glue, casein or egg yolk [1]. When these kind of paintings are exposed to natural or accelerated conditions, they can suffer different alteration processes that depend on the nature of the binder and pigment, and on the interaction between them. Also, these alteration processes will be different attending to the environment of exposure, e.g. marine influence or/and presence of pollutants from traffic and industrial activities.

On the one hand, the painting surface may have different roughness and colorimetric characteristics depending on the binder, and subsequently the paint response to ageing will be different [2]. As regard to inorganic pigments, they can suffer chemical alteration through the interaction with moisture and air components (O_2, NO_x, CO_2, SO_2, SO_3 and H_2S), resulting in undesirable colour changes [3,4]. Indeed, the exposure to O_2, atmospheric sulphur-containing compounds, or CO_2, can lead to chemical alterations and mineralogical transformations of pigments, such as minium to plattnerite (PbO_2) [5], lead-based pigments to black galena (PbS) [6], or azurite to copper sulphates chlorides [7]. Also, the interaction between metallic pigments (e.g. Zn, Mn or Cu based pigments) with a specific binder may result in the production of metal soaps in the surface of the painting, modifying its appearance [8].

One of the most immediate visible effect derived from the impact of the environment in an artistic painting is its colour change. Thus, the analysis of the paints in the visible and infrared spectrum would allow monitoring their compositional changes, and therefore identifying the deterioration processes that subsequently would be investigated with other analytical techniques. Hence, colorimetric methods applied to monitor colour changes of paint mock-ups subjected to accelerated or natural aging tests, are a potential tool in preventive conservation. Nevertheless, these methods, commonly used in the monitoring of deterioration of materials such as rocks, plastics and wood [9,10], are poorly developed in the case of pictoric cultural heritage [4].

Moreover, in studies that evaluate colour variation of materials subjected to natural or artificial environments, the colour analysis is performed quantitatively by calculating the colorimetric differ-

* Corresponding author.
E-mail address: ipozo@uvigo.es (J.S. Pozo-Antonio).

http://dx.doi.org/10.1016/j.measurement.2017.06.037
0263-2241/

ences in the colour spaces most used (CIE L*a*b* and CIE L*C*h) [11,12]. However, this type of descriptive approach is not satisfactory to deal with, for example, the study of colour variation when multiple variables or factors of variation are considered, as well as in time series studies [13].

This study is based on the evaluation of the suitability of two different statistical approaches (vectorial and functional analyses) to identify trends and similarities in colour changes of several tempera mock-ups paints during thirteen months. The samples were subjected to a natural urban atmosphere characterized by an important marine and industrial influence. Binary paint mock-ups were prepared by mixing an inorganic pigment with either egg yolk or rabbit glue binder. Seven historic pigments with different grain size were used. In the outdoor test performed in this study, the variability in composition of the paints (related to pigment and binder) and texture (pigment grain size) implies the existence of a large number of variables or factors of variation which requires the application of a statistical methodology that also can be adapted to the analysis of colour measures depending on time.

2. Materials and methods

2.1. Tempera mock-ups

As Table 1 shows, thirty-six samples (tempera paint mock-ups) composed of one out of seven pigments (chalk, gypsum, white lead, haematite, cinnabar, azurite and lapis lazuli) with different grain sizes mixed with either egg yolk or rabbit glue binder were prepared according to Old Master recipes to obtain standards similar to those used by medieval artists [14]. The pigments were supplied by Kremer Pigments GmbH & Co. (Madrid, Spain), except CIN-ST that was supplied by Caremi Pigmentos (Sevilla, Spain). The white pigments were chalk ($CaCO_3$), gypsum ($CaSO_4{\cdot}2H_2O$) and white lead or cerusite ($PbCO_3$). The red pigments were haematite (Fe_2O_3) and cinnabar (HgS) and the blue pigments azurite ($Cu_3(CO_3)_2(OH)_2$ and lapis lazuli or lazurite ($Na_3Ca(Al_3Si_3O_{12})S$. Different grain sizes of the pigments were used as is shown in Table 1. Taking into account a previous work [4] in which no correspondence between the information provided by the supplier and that experimentally obtained in the laboratory, particle size of the commercial pigments used in this work was obtained using a Master sizer 2000LF laser diffraction instrument (Malvern Instruments). The pigment size by the supplier and experimental data is shown in Table 1.

The binders used were rabbit glue from Kremer Pigments GmbH & Co. (Madrid) and egg yolk (purchased in the market) to prepare lean (rabbit glue) and fatty (egg yolk) tempera paints in a ratio pigment: binder needed to obtain a workable tempera paint. The paint mock-ups were prepared applying traditional recipes of the Renaissance and Middle Ages, considering organoleptic parameters, because considering the nature and the size of the pigment, different binder quantities are required [14,15]. Thus, the pigment was mixed with binder (T < 50 °C) in order to achieve an adequate consistency. The consistency was found adequate when droplets formed at the tip of the brush would not fall off easily and the achieved viscosity of the paint allowed the brush to adequately slip on the surface of the substrate [14,15]. Then, several layers of paint were applied by brush to 76 × 26 × 1 mm-glass slides; the application of the successive layers was performed after the complete drying of the previous one. In order to ensure the drying, the samples were left forty-eight hours subjected to the laboratory conditions and also to confirm that, a dry brush did not drag paint [1].

Then, the following analyses were performed: (1) macroscopic characterization by the visualization under a stereomicroscope (SMZ 1000, Nikon) using reflected light; (2) mineralogical composition using X-ray Diffraction (XRD, X'Pert PRO PANalytical B.V using Cu-Kα radiation, Ni filter, 45 kV voltage, 40 mA intensity and a goniometer speed 0.05° 2θ s^1) (Table 1) and (3) molecular composition by Attenuated Transmittance Reflectance -Fourier transform infrared spectroscopy (ATR-FTIR; Thermo Nicolet® 6700); infrared (IR) spectra were recorded at a 2 cm^{-1} resolution over 100 scans from 500 to 4000 cm^{-1} and, in the case of cinnabar and haematite paintings, also in the far region (from 50 to 500 cm^{-1}).

2.2. Atmospheric exposure conditions and colour monitoring

The paint mock-ups were placed in an open balcony faced to the Atlantic Ocean in Vigo (Galicia, NW Spain) (Fig. 1) during thirteen months (December 2014 to January 2016). Vigo (population 300,000) is a major Atlantic port city in terms of industrial, commercial, fishing and shipbuilding activities. Galicia has, according to FAO's agro-ecological zoning, a humid sub-tropical climate, with rainy winters (1200 mm rainfall) [16,17]. During the thirteen months, the samples faced N receiving the direct solar irradiation, were subjected to an accumulated precipitation of 1200 mm. The average RH was ~80% and the average annual temperature was 14 °C, with a T_{max} of 33.10 °C (July 2015) and a T_{min} of 5.90 °C (February 2015) [18].

The ambient of exposure in this place is characterized by a high influence of sea spray and atmospheric pollutants derived from traffic and industrial activity [19]. The main inorganic contaminants in this site are chloride (from marine origin), SO_2 (derived from both anthropogenic sources and marine aerosol) and, in a lesser extent, nitrates (derived from farming) [19]. According to Silva et al., over 50 % of the SO_2 in bulk depositions in Galician coastal cities are of marine origin [20].

Table 2 shows the air quality data [18] corresponding to the two most representative months during the period of study (December 2014 to January 2016); they exhibited the more extreme values comparatively to the rest of the months. The concentration of SO_2, CO and the particulate matter with 10 mm average size (PM_{10}) kept approximately constant during the thirteen months, however the concentrations of the other pollutants (NO, NO_2, NO_x and O_3) showed remarkable difference over the time; NO, NO_2 and NO_x – concentrations were higher for the winter, while for O_3, the higher concentrations were registered during spring and summer months.

At the beginning of the exposure test and every fifty days during the thirteen months of the trial, the colour of each paint mock-up was characterized by means of a Minolta CM-700d spectrophotometer equipped with the software CM-5100W SpectraMagic NX and expressing the colour in the colour spaces CIE L*a*b* and CIE L*C*h [21]. In the space CIE L*a*b*, the coordinate L* represents the lightness which varies from 0 (absolute black) to 100 (absolute white), and the coordinates a* and b* expressed the colour wheel, take values of +a* (red) to −a* (green) and +b* (yellow) to −b* (blue). In the space CIE L*C*h, the L* coordinate is the one described for space CIE L*a*b*, the C^*_{ab} parameter expressed the chroma or colour saturation and its value corresponds with the expression $C^*_{ab} = [(a^*)^2 + (b^*)^2]^{1/2}$ and h_{ab} expressed the hue and is calculated by means the expression $h_{ab} = tan[1 - (a^*/b^*)]$. The measurements were made with the Specular Component Included (SCI), using a spot diameter of 3 mm, a D65 lamp as illuminant and an observer angle of 10°. A total of eighteen random measurements for the thirty-six samples were performed.

The colour difference is defined as the numerical comparison of the sample with the reference. Colour coordinate differences (ΔL*,

Table 1
Information of the inorganic pigments: manufacturer code, pigment size by the supplier (μm), authors code, particle size range (μm) experimentally obtained and mineralogical composition of the temperas obtained experimentally.

Manufacturer pigment code	Supplier pigment size (μm)	Authors pigment code	Authors grain size range (μm)	Authors mineralogical composition	
White temperas					
Calcite 58720	20	CA-EF	0.25–100	Egg yolk	Calcite, Dolomite, Quartz
				Rabbit glue	Calcite, Portlandite, Quartz
White San Giovanni 11415	120	CA-C	0.25–120	Egg yolk	Portlandite, Calcite
				Rabbit glue	Portlandite, Calcite
White San Giovanni 11416	120–1000	CA-EC	0.3–250	Egg yolk	Portlandite, Calcite
				Rabbit glue	Portlandite, Calcite
Gypsum natural 58300 Selenite (Terra Alba)	80% < 20 18% < 25 1.9% < 32 0.1% < 40	G-EF	0.2–75	Egg yolk	Bassanite
				Rabbit glue	Gypsum, Anhydrite, Bassanite
Gypsum alabaster 58343	85% < 40	G-F	1–160	Egg yolk	Bassanite, Anhydrite
				Rabbit glue	Bassanite
Gypsum alabaster plaster Italian 58340	<75	G-M	0.2–85	Egg yolk	Gypsum, Anhydrite, Bassanite
				Rabbit glue	
KREMER White lead 46000	<45	WL	0.1–10	Egg yolk	Hydrocerussite, Cerussite
				Rabbit glue	Hydrocerussite, Cerussite
Red temperas					
Haematite, 48651	1.5	HE	0.3–17	Egg yolk	Haematite, Dolomite, Quartz
				Rabbit glue	Haematite, Dolomite, Quartz
Cinnabar standard PR 106[1]	<120	CIN-ST	2–25	Egg yolk	Cinnabar, quartz
				Rabbit glue	Cinnabar, quartz
Cinnabar, 10624	<20	CIN-EF	0.4–40	Egg yolk	Cinnabar, quartz
				Rabbit glue	Cinnabar, quartz
Cinnabar, 10627	50–63	CIN-M	15–90	Egg yolk	Cinnabar, quartz
				Rabbit glue	Cinnabar, quartz
Cinnabar dark, 10628	63–100	CIN-C	40–130	Egg yolk	Cinnabar, quartz
				Rabbit glue	Cinnabar, quartz
Blue temperas					
Azurite standard, Deep greenish blue, 0200	<120	AZ-ST	0.2–55	Egg yolk	Azurite, Quartz, Malachite
				Rabbit glue	Azurite, Quartz, Malachite
Azurite MP sky blue, light greenish blue 10207	<38	AZ-EF	4–90	Egg yolk	Azurite, Quartz, Malachite
				Rabbit glue	Azurite, Quartz, Malachite
Azurite MP Pale, Light blue 10206	38–63	AZ-M	20–110	Egg yolk	Azurite, Quartz, Malachite
				Rabbit glue	Azurite, Quartz, Malachite
Azurite MP Deep Dark blue, 10204	63–80	AZ-C	25–180	Egg yolk	Azurite, Quartz, Malachite
				Rabbit glue	Azurite, Quartz, Malachite
Azurite MP extra deep, Intense dark blue 10203	80–100	AZ-EC	20–280	Egg yolk	Azurite, Quartz, Malachite
				Rabbit glue	Azurite, Quartz, Malachite
Lapis lazuli natural pale, 10540	<80	LAP	0.6–95	Egg yolk	Lazurite, Calcite, Diopside
				Rabbit glue	Lazurite, Calcite, Diopside

Note: EF = extra fine; C = coarse; EC = extra coarse; M = medium; ST = standard.

Δa^* and Δb^*) and the global colour change (ΔE^*_{ab}) were calculated as follows:

$$\Delta L^* = L^*_x - L^*_0$$

$$\Delta a^* = a^*_x - a^*_0$$

$$\Delta b^* = b^*_x - -b^*_0$$

$$\Delta E^*_{ab} = \left[(\Delta L^*)^2 + (\Delta a^*)^2 + (\Delta b^*)^2\right]^{1/2}$$

The colour of the original samples (before to be exposed to the elements) was considered the reference value (L^*_0, a^*_0, b^*_0). Therefore, the higher the ΔE^*_{ab} the greater the global colour change respect to the original colour. Once the test was finished, the paint mock ups were again visualised under stereoscopic microscopy and analysed by means of XRD and ATR-FTIR spectroscopy, following the procedures explained in Section 2.1.

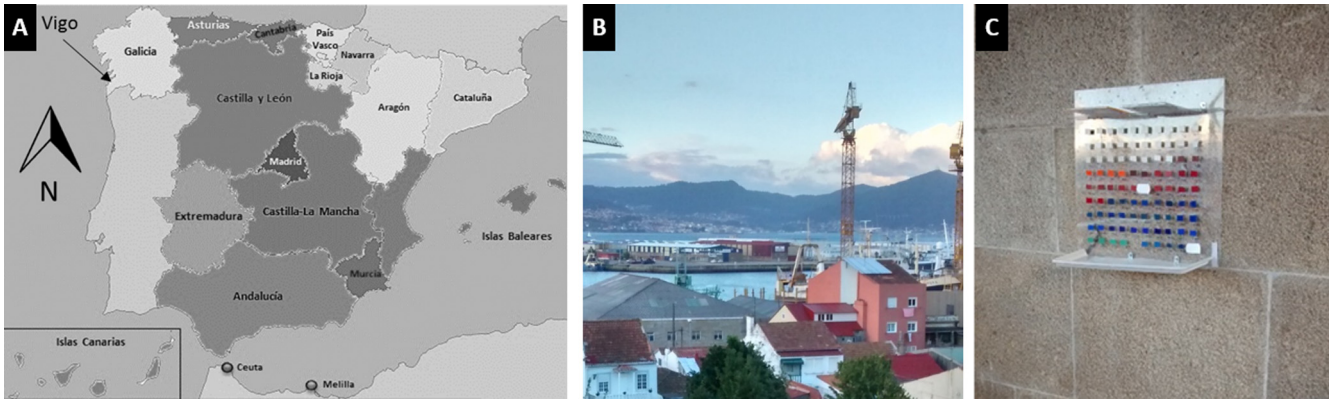

Fig. 1. Location of the paint mock-ups in Vigo, NW Spain (A) and view (B) from the balcony where the paint mock-ups panel (C) was exposed to the environment.

Table 2
Average air contamination and particulate matter (PM_{10}) concentration ($\mu g\ m^{-3}$) during the two more representative months of spring and winter in the city center of Vigo during the study period [18].

Months	SO_2	CO	NO	NO_2	NO_x	O_3	PM_{10}
May 2015	3.91	0.11	2.03	8.54	11.09	63.81	17.88
November 2015	3.38	0.16	21.41	35.41	68.10	28.20	18.59

2.3. Statistical analysis of colour variations

In order to investigate the evolution of the colour changes of the paint mock-us during the exposure test, and to statistically identify differences in the behaviour among the paintings, regarding the type of the binder and the pigment, two statistical procedures were applied, i.e. a vectorial analysis and a functional analysis. In both type of analyses, three variables were analysed: ΔL^*, ΔC^*_{ab} and ΔE^*_{ab}. Differences between the values of these variables obtained for rabbit glue tempera and the values for the same variables obtained for the egg tempera were used as data sample. Thus, the proposed analyses, both vector and functional, focus on evaluating the differences in behaviour during the exposure among each family colour tempera depending on the nature of the binder (egg yolk and rabbit glue).

The classical vector analysis was performed using a box and whiskers plots whose main characteristics are: (1) the boundaries of each box correspond to the first and third quartile of the sample; (2) the centre line corresponds to the median; (3) the ends of the whiskers (dotted lines) identify the extreme values, 1.5 times the interquartile range from the ends of the box; (4) outliers, i.e. those elements of the paint sample that fall outside of these extremes (identified by a cross). This type of analysis is very useful to analyse two types of features [13]:

- Trend: The position of the box as a whole along the time instants analysed, allows determining whether the sample shows a trend regarding the considered parameter.
- Homogeneity: Analysing the width of the box at each time instant, it is possible to determine the evolution of the homogeneity of the behaviour within the sample over time.

The functional analysis allows treating a set of data as continuous measurements, transforming an initial vector problem in a functional problem. This allows analysing the trend and periodicity of measurements without considering possible measurements errors of discrete character, which may be considered insignificant due to their origin and occurrence. Functional approach has also an added advantage regarding the vast majority of criteria outlier detection; thus, it does not require a normally distributed sample data or a transformation needed for that purpose.

More in detail, given a set of observations $x(t_j)$ contained in a set of n_p points where t_j represents each instant of time and n_p the number of observations ($j = 1, 2, \ldots, n_p$), all observations can be considered as discrete observations of a function x(t) in F, where F is a functional space. For convenience, the following expansion is considered for recording function:

$$x(t) = \sum_{k=1}^{n_b} c_k \phi_k(t)$$

Which c_k represents the coefficients of the function x(t) with respect to the set of selected basic functions.

The first phase of functional analysis is the process of smoothing which allows solving the following problem regularization [22]:

$$\min_{x \in F} \sum_{j=1}^{n_p} \{z_j - x(t_j)\}^2 + \lambda \Gamma(x)$$

Once the data are transformed into functional data, they are already prepared for the jump to the second phase, in which they can be analysed to detect outliers using the concept of functional depth. This concept provides a sorting criteria for a set of points contained in a Euclidean space, from its centre to the periphery. According to this criterion, the nearest to a point the centre is, the greater its depth is. In multivariate analysis, the depth is usually used as a measure of the centrality of a point from a point cloud [23]. Considering the functional problem [24], the depth represents the centrality of certain curve contained in a set of curves. Therefore, based on the functional depth, those functions with lower depths are identified as outliers.

After the calculation of the functional depths, a third phase is performed, which consists on the analysis of the outliers of the sample. For this, the cutoff value (C) is estimated from bootstrapping approximation method. Cuttoff value was selected so that the percentage of observations misidentified as outliers was about 1% [25].

3. Results and discussion

3.1. White paints mock-ups

Fig. 2 depicts the evolution, following the vectorial and functional approaches, of ΔL^*, ΔC^*_{ab} and ΔE^*_{ab} of the white tempera mock-ups during the exposure test. The graphs of the vectorial analysis indicate that the change in the coordinate L^* (Fig. 2A) was slightly more pronounced in egg yolk-based paintings, whereas the change in C^*_{ab} (Fig. 2B) was more pronounced in rabbit glue-based paintings. Globally, ΔE^*_{ab} was more pronounced in samples made with egg yolk (Fig. 2C), which indicate the greater contribution of the variation of the L^* coordinate to the ΔE^*_a on this colour family of tempera paints.

Differences in the behaviour of rabbit glue and egg yolk tempera samples with respect to L^* and ΔE^*_{ab} were not statistically significant; however, vector analysis did detect significant differences relative to C^*_{ab} of one type of white tempera, GM (Fig. 2B). This different behaviour corresponds to the rabbit glue-based G-M tempera; thus, if only the data of the C^*_{ab} variation corresponding to the paintings made with rabbit glue is graphically represented in the vectorial approach (Fig. 2D), it can be observed that the rabbit glue-based G-M paint suffer, in three moments of the test, an intense decrease in C^*_{ab} compared to the rest of the samples made with the same binder. Similarly, the vector analysis applied on white tempera paintings with rabbit glue detected a statistically different increase in the C^*_{ab} of the CA-EC tempera paint respect to the rest of the samples.

The atypical behaviour of the rabbit glue-based G-M paint regarding C^*_{ab} was confirmed by the functional analysis, although not that of the CA-EC paint (Fig. 2E). The atypical behaviour of the rabbit glue-based G-M paint is observed in Fig. 2F: C^*_{ab} decreased at 55 days after the beginning of the outdoor exposure, remaining constant throughout the test, contrary to the other tempera paints of this group, in which the decrease in the C^*_{ab} was lower and did not show a clear relationship with the exposure time.

Stereomicroscope micrographs showed that for the white paint mock-ups, the outdoor exposure caused a smoothing of the roughness of their surfaces (Fig. 3). These changes are similar in all the samples regardless the binder used, and no macroscopic differences were observed among temperas made with each type of pigment which could explain the different behaviour of the G-M and CA-EC paints. Regarding the composition, mineralogical changes were detected after the exposure test in calcite and gypsum temperas. Instead the white lead tempera did not showed compositional changes. In calcite ($CaCO_3$) temperas made with both binders, the complete transformation of portlandite ($Ca(OH_2)$) to calcite was produced, being remarkable the fact that vaterite (a polymorph of $CaCO_3$) formed in CA-C and CA-CE tempera paints. In the gypsum ($CaSO_4{\cdot}2H_2O$) paintings, mineralogical changes were more intense in paintings made with rabbit glue: bassanite ($CaSO_4{\cdot}1/2H_2O$) was partially transformed into gypsum, being also noteworthy the crystallisation, after the exposure time, of anhydrite ($CaSO_4$). In any case, mineralogical changes suffered by the rabbit glue-based G-M paint, which was identified as an outlier by the functional statistic approach, were similar to the other paints made with gypsum. Thus, an influence on the colour changes and on the evolution of the mineralogical changes of the pigments is discarded.

FTIR analyses did no either provide conclusive results about the reason for the different behaviour of the samples during the exposure test, especially between G-M and CA-EC paintings and the others white paints. For comparative purposes, Fig. 4A depicts the spectra of a white tempera whose behaviour was not atypical (G-EF) and Fig. 4B shows the FTIR spectra of the G-M tempera (detected as an outlier by means of functional statistical analysis). FTIR allowed detecting the mineralogical changes described previously. Regarding the binders, this technique confirmed that the outdoor exposure produced, in general terms, a slight decrease on the intensity of the bands. In the rabbit glue-based paintings, this decrease mainly affected the FTIR bands at 1630 cm^{-1} (assigned to $\upsilon(C=O)$ stretching from amide I), at 1520 cm^{-1} (assigned to $\upsilon(CN)$ stretching and $\nu(NH)$ bending from amide II), and bands between 1400 and 1000 cm^{-1} (collagen absorption features attributed to CH_2 wagging, CH_3 deformation, C–N stretching and C–OH stretching) [26–28]. In the egg yolk-based paintings, the FTIR bands that suffered the greatest decline were those at 2920 cm^{-1} ($\nu_{AS}(CH_2)$ stretching from long chain fatty acids), at 2850 cm^{-1} ($\nu_S(CH_2)$ stretching from long chain fatty acids), at 1650 cm^{-1} ($\upsilon(C=O)$ stretching from amide I), and at 1550 cm^{-1} ($\nu(N–H)$ bending from amide II) [8,29]. All these changes were observed with the same intensity in all the white paintings, regardless the pigment nature and the grain size. Finally, no relationship was found between the statistical differences detected on the evolution of the colour parameters and the binder percentage of the tempera samples.

3.2. Red paintings mock-ups

Fig. 5 shows the evolution, following the vectorial and functional approaches, of ΔL^*, ΔC^*_{ab} and ΔE^*_{ab} of the red tempera mock-ups during the outdoor exposure test. Contrary to those obtained in the group of white paints, the variation of the L^* coordinate is more pronounced in rabbit glue paintings (Fig. 5A), while the change in the chroma is more pronounced in egg yolk (Fig. 5B). The global colour change ΔE^*_{ab} is more pronounced for rabbit glue paints (Fig. 5C), which indicate that luminosity is once again the coordinate that most contributes to the overall colour change of red paints. Although the vector analysis did not define any atypical behaviour for the red tempera paints, the functional analysis identifies an atypical behaviour in the HE paint (Fig. 5D).

The vectorial analysis performed separately for each group of paints as a function of the binder revealed significant differences in the evolution of ΔE^*_{ab} of the HE tempera made with egg yolk (Fig. 5E), which was also confirmed by the functional approach (Fig. 5F). This different evolution of ΔE^*_{ab} in the egg yolk-based HE tempera paint is depicted in Fig. 5 G-I, where it can be seen that ΔL^* of this sample suffered an increase in luminosity from the time instant number 4 (220 days of exposure) to the end of the thirteen months of outdoor exposure, conversely to what occurs in the other paints made with the same binder, whose ΔL^*suffered a slight decrease.

After the exposure test, stereomicroscopy allowed detecting, in general terms, a remarkable decrease of colour intensity in the temperas (colour becomes paler), mainly in the egg yolk- based HE paint (Fig. 3) where the colour also became lighter. These changes in the appearance of the egg yolk-based HE tempera is in agreement with the modifications of the coordinates L^*, C^*_{ab} and the global colour change ΔE^*_{ab} shown in Fig. 5. However, the statistical differences detected seems to be not related with the deterioration of the pigments, since XRD did not detected mineralogical changes neither in HE nor in CIN tempera paints.

The stability of the pigments during the exposure test was also confirmed by FTIR, though significant changes were recognised in the binders. In all the rabbit glue-based red tempera, several bands assigned to rabbit glue suffered a notable decrease after the outdoor exposure (or even disappeared). The more affected FTIR bands corresponded to the peptide linkage, showing bands at ~3300 cm^{-1} and at 1650 cm^{-1} and 1550 cm^{-1}, assigned to amide I and amide II respectively. These modifications were previously reported on similar tempera paint mock-ups also outdoor exposed

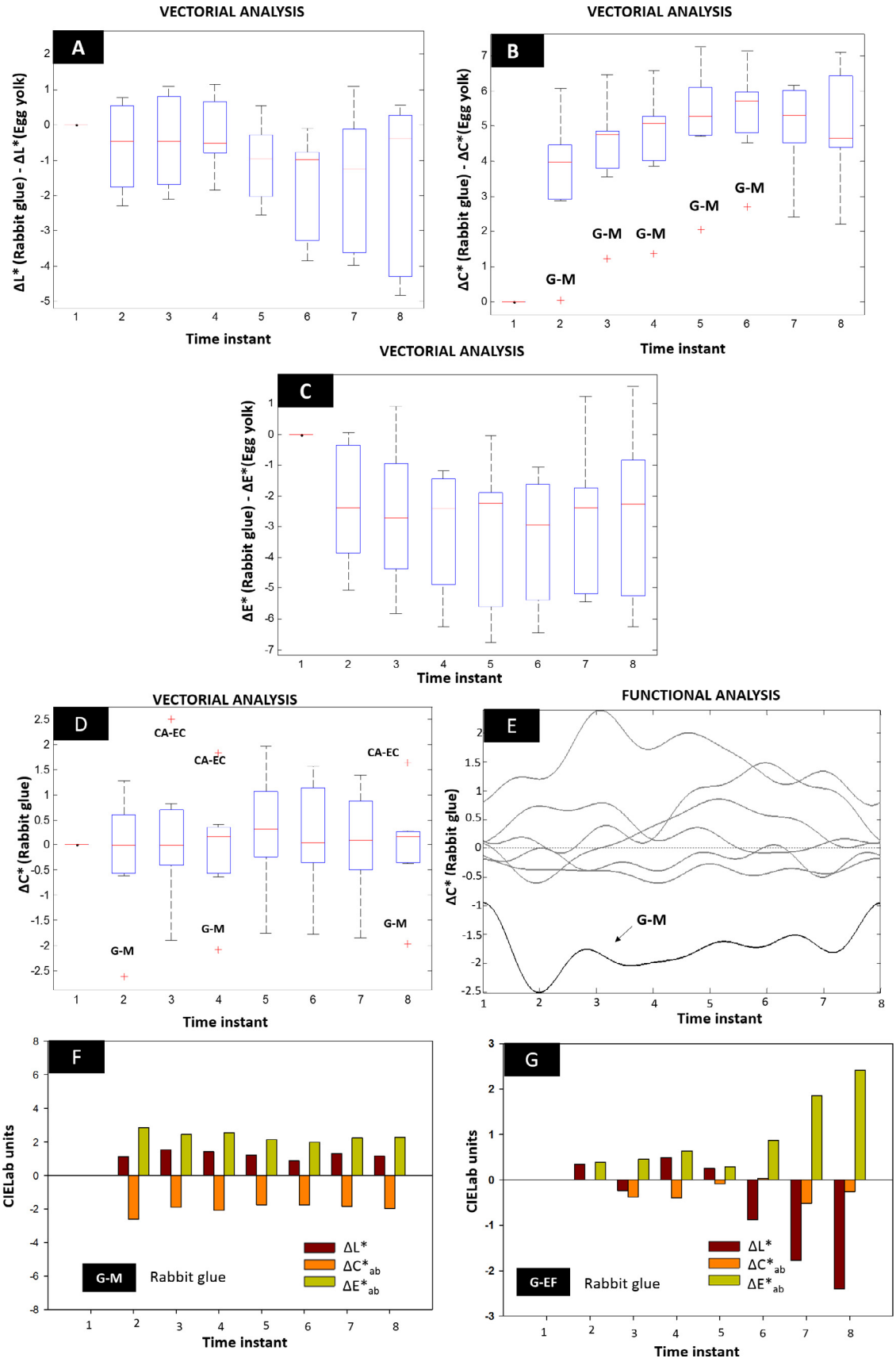

Fig. 2. A–C: Vectorial (box plots) analysis for variable difference between rabbit glue and egg yolk white tempera data. A: Variable = ΔL^*; B: Variable = ΔC^*_{ab}; C: Variable = ΔE^*_{ab}. D: Vectorial (box plots) for ΔC^*_{ab} rabbit glue white tempera data. E: Functional analysis for ΔC^*_{ab} rabbit glue white tempera data. F: ΔL^*, ΔC^*_{ab}, ΔE^*_{ab} over time for G-M painting with rabbit glue (identified as an outlier by the functional analysis). G: ΔL^*, ΔC^*_{ab}, ΔE^*_{ab} over time for G-EF paint with rabbit glue.

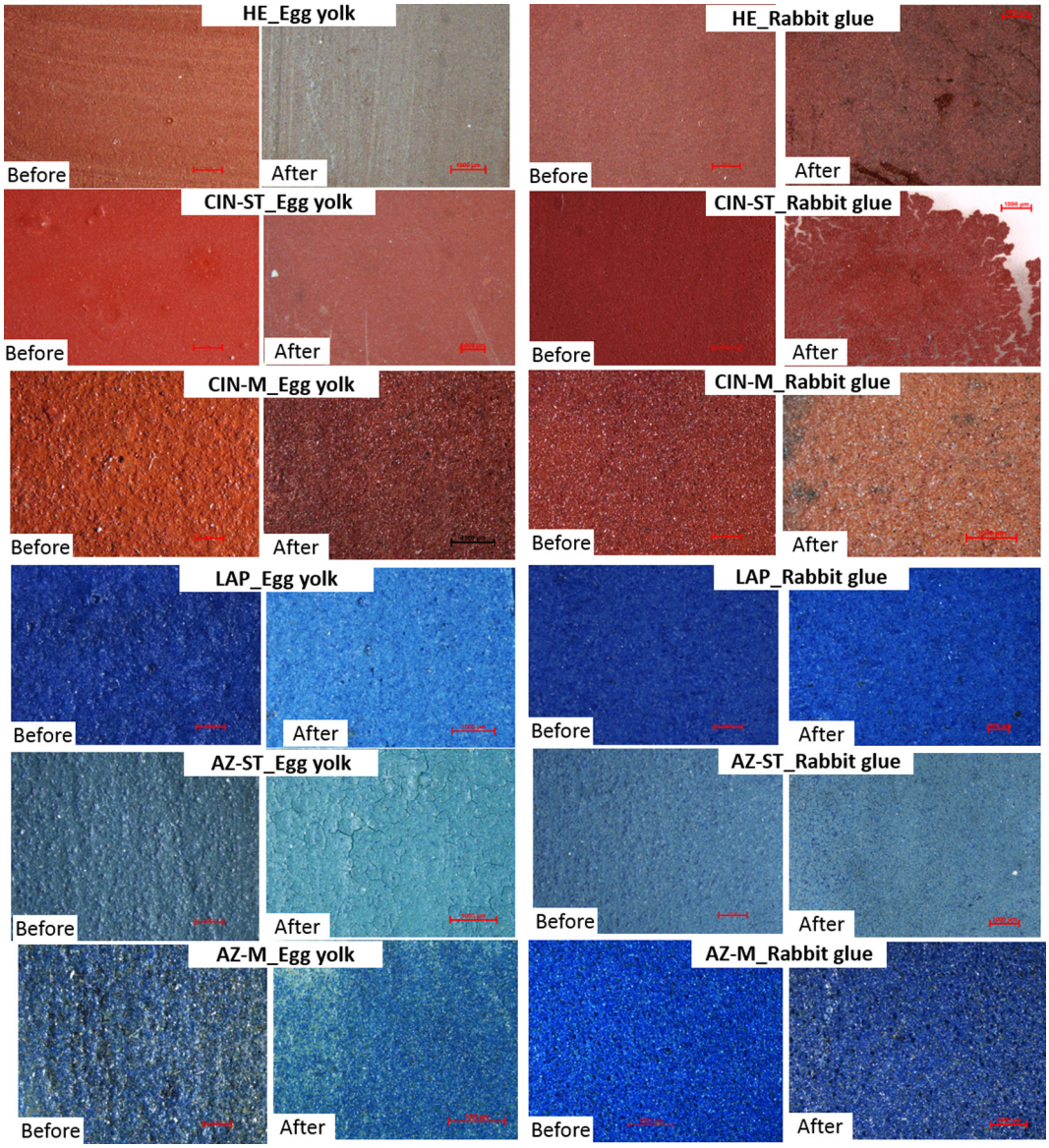

Fig. 3. Micrographs taken with stereomicroscope of several egg yolk and rabbit glue tempera paintings before and after the exposure to outdoor environment.

under different urban atmosphere [4]. Conversely to that occurred in rabbit glue, the egg yolk FTIR bands remained unaltered in all the red tempera except in the egg yolk- based HE tempera, which was the sample identified as an outlier for the functional analysis.

Fig. 6A depicts the FTIR spectra of the CIN-M paints made with either egg yolk or rabbit glue binder, as an example of the general behaviour of the red paintings, and Fig. 6B shows the FTIR of the HE tempera which was identified as an outlier for the functional analysis. In addition to the modification on the rabbit glue FTIR bands (common in all the red tempera paints), it is observed that in the egg yolk-based HE tempera, the absorption bands assigned to esters ($2920\ cm^{-1}$, $2850\ cm^{-1}$, $1732\ cm^{-1}$) suffered an intense decrease. This effect, as reported by Meilunas et al. and Mazzeo et al. could probably be due to the formation of free fatty acids groups derived from a partial hydrolysis of the lipidic fraction [8,30]. Thus, the atypical behaviour of the egg yolk-based HE tempera regarding ΔL^* could be assigned to the binder deterioration. Therefore, the loss of the egg yolk binder during the exposure test leaves the haematite pigment uncovered, favouring a variation in its luminosity, as similarly found by Cardell et al. in azurite-based tempera mock-ups [4].

3.3. Blue paintings mock-ups

The evolution of the colour parameters for the blue tempera mock-ups during the exposure test, following vectorial and functional statistical approaches, is shown in Fig. 7. The vectorial analysis indicates that the changes of the three parameters evaluated were more pronounced in the egg yolk-based paintings than in those made with rabbit glue (Fig. 7A–C). The vectorial analysis detected significant differences in the behaviour of three temperas. Thus, AZ-M and LAP tempera paints behaved atypical with respect to ΔL^* (Fig. 7A), AZ-ST tempera showed an atypical behaviour in relation to the variation of C^*_{ab} (Fig. 7B), and AZ-ST and AZ-M tempera paints did so with respect to ΔE^*_{ab} (Fig. 7C). However, functional analysis showed only statistically atypical behaviours in LAP and AZ-ST tempera paints (Fig. 7D and E).

The vectorial analysis performed separately for each group of paints, as a function of the binder, revealed no significant differences among the tempera mock-ups made with rabbit glue. Conversely, this statistical approach detected statistically different behaviours in several tempera paints made with egg yolk (Fig. 7F and G). LAP and AZ-M tempera paints showed atypical behaviours

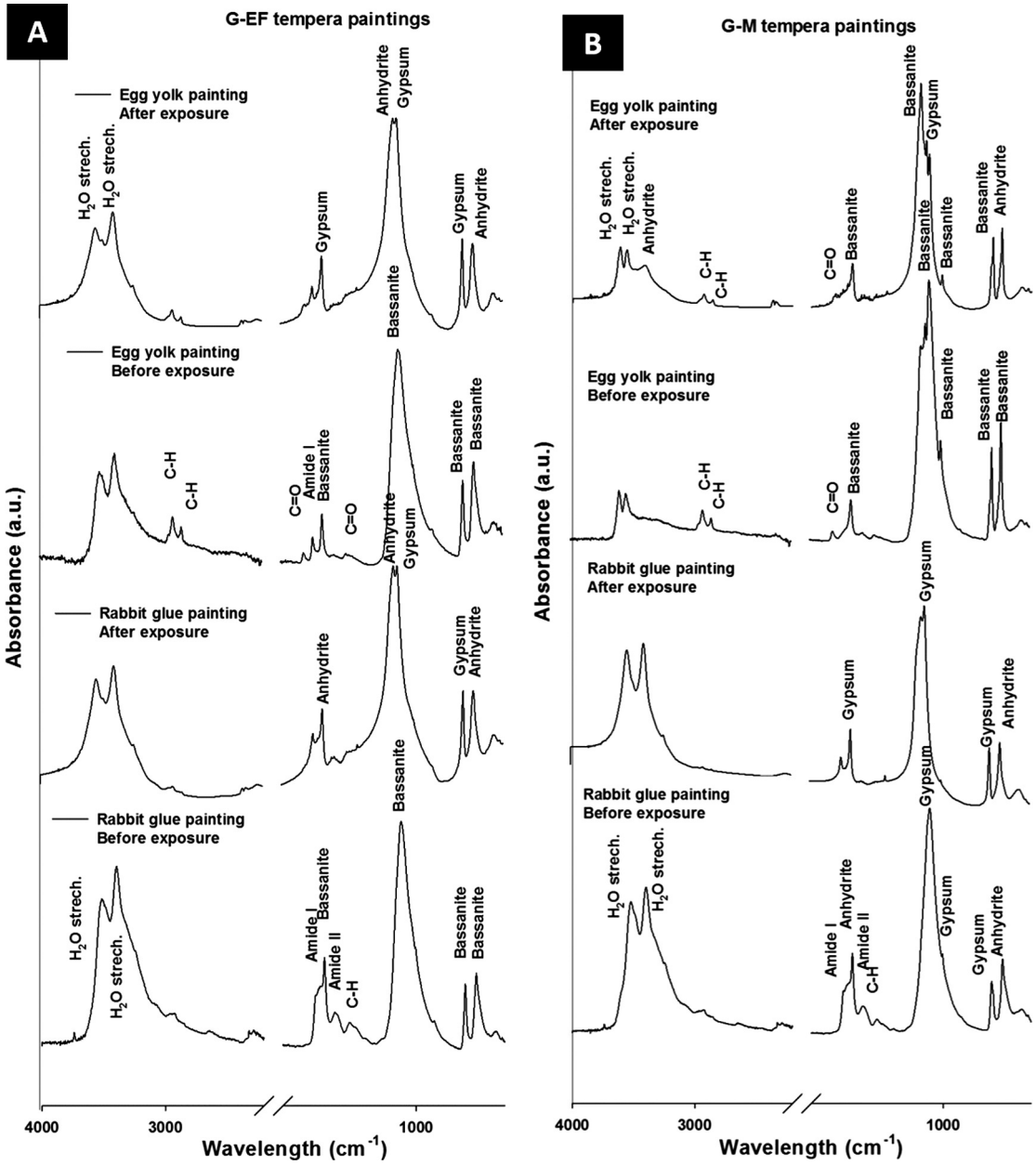

Fig. 4. FTIR (absorbance) spectra of some white paint mock-ups with either rabbit glue or egg yolk before (initial) and after (final) the exposure to outdoor environment. A: G-EF painting; B: G-M paintings.

regarding ΔL^*. Thus LAP tempera suffered a greater increase of L^* than the other tempera paints, whereas AZ-M showed a decrease on L^*. As well the AZ-ST tempera showed an atypical behaviour regarding ΔC^*_{ab} showing a lower increase in chroma than the other tempera paints. Functional analysis confirmed only atypical behaviours for LAP samples regarding ΔL^* and AZ-ST regarding ΔC^*_{ab} (Fig. 7H and I).

The nature of such atypical behaviours is shown in Fig. 8, where the evolutions of ΔL^*, ΔC^*_{ab} and ΔE^*_{ab} of the egg yolk-based tempera paints are represented. It is observed that in AZ-ST egg yolk tempera L^* underwent a variation with the exposure time, in contrast to other tempera composed of azurite pigment with different grain size. Likewise, the egg yolk-based LAP paint suffered a greater ΔL^* than the other blue tempera paints. In general terms, ΔC^*_{ab} is ≥ 5 for all the blue egg yolk-based tempera paints, except for the AZ-ST, which was identified as an outlier by the functional analysis.

Stereomicroscopy allowed detecting that the colour change on azurite paintings was more pronounced than that occurred on LAP paintings (Fig. 3). Among the azurite paint mock-ups, colour changes were higher in the egg yolk-based paints than in the rabbit glue-based paints (Fig. 3). As well it was found that the egg yolk-based AZ-ST paint developed a higher degree of fissuration after the exposure test.

The XRD results revealed that no mineralogical transformation took place in the blue paints mock-ups. Thus, azurite, malachite and quartz were the minerals detected in the azurite-based paints, and lazurite, calcite and diopside the minerals found in the LAP paints. However clay minerals (layer-lattice silicates) were detected on the surface of several paint mock-ups, which were considered atmospheric dust.

FTIR spectra obtained before and after the exposure test allowed us to confirm variations on the bands assigned to the bin-

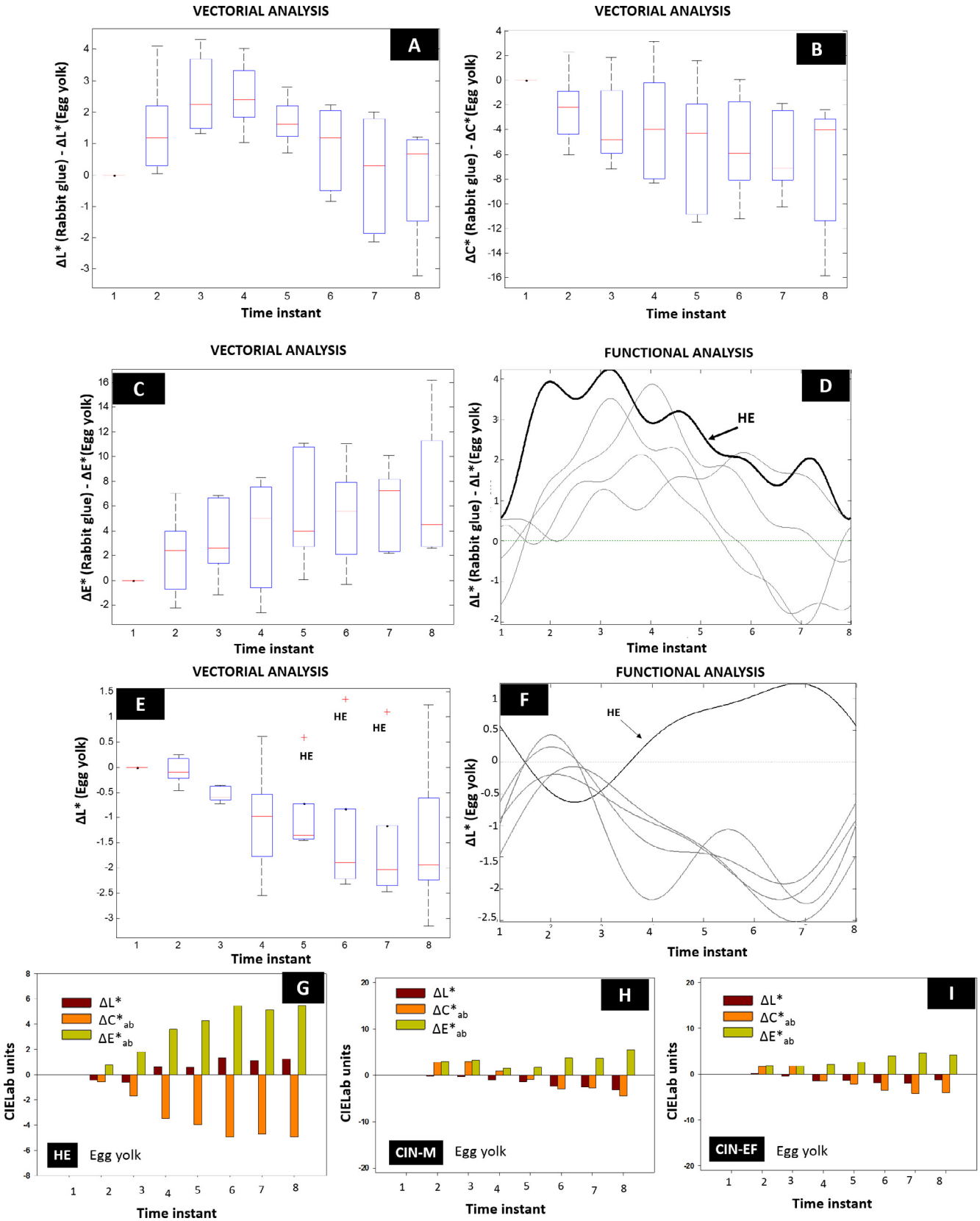

Fig. 5. A–C: Vectorial (box plots) analysis for variable difference between rabbit glue and egg yolk red tempera data. A: Variable = ΔL^*; B: Variable = ΔC^*_{ab}; C: Variable = ΔE^*_{ab}. D: Functional analysis for ΔL^* difference between rabbit glue and egg yolk red tempera data. E: Vectorial (box plots) analysis for ΔL^* difference data on egg yolk red tempera. F: Functional analysis for ΔL^* data on egg yolk red tempera. G: ΔL^*, ΔC^*_{ab}, ΔE^*_{ab} variations over time for egg yolk-based HE paint (identified as an outlier by the functional analysis). H: ΔL^*, ΔC^*_{ab}, ΔE^*_{ab} variations over time for egg yolk-based CIN-M paint. I: ΔL^*, ΔC^*_{ab}, ΔE^*_{ab} variations over time for egg yolk- based CIN-EF paint.

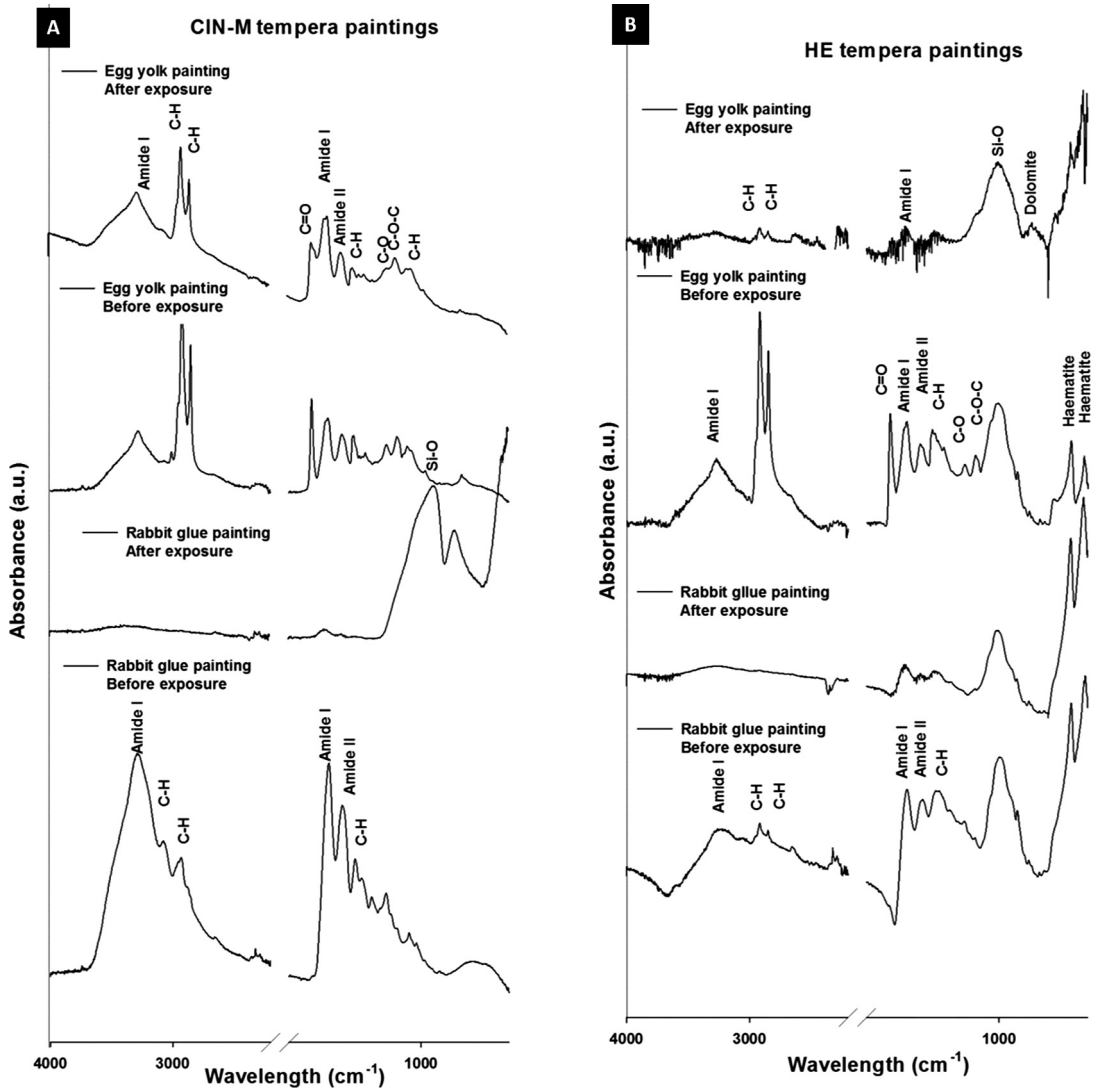

Fig. 6. FTIR (absorbance) spectra of some red paintings with rabbit glue and egg yolk before (initial) and after (final) the outdoor exposure test. A: CIN-M tempera paintings showing the general trend for the CIN paintings. B: HE tempera paintings.

ders, as also occurred for the red paintings. Fig. 9 depicts the FTIR spectra for the different blue paint mock-ups made with either egg yolk or rabbit glue. Specifically, Fig. 9A shows the AZ-M sample which represents the general results obtained for most of the blue tempera paint, while Fig. 9B and C shows the LAP and AZ-ST samples respectively, which are both identified as outliers by means of functional analysis. In general terms, it seems that rabbit glue binder was more affected by the outdoor exposure that the egg yolk binder, since it was found that the rabbit glue FTIR bands decreased in all the blue paint mock-ups. However, in the egg yolk- based LAP paint (identified as outliers by means the statistical analyses regarding to the ΔL^* behaviour), a decrease on the FTIR absorption bands assigned to egg yolk was confirmed (Fig. 9B).

Conversely to the egg yolk-based LAP paint, the FTIR bands of the both binders in the AZ-ST samples did not suffer any change after the exposure test (Fig. 9C), although AZ-ST pigment was identified as outlier for the functional analysis regarding ΔC^*_{ab} for the egg yolk tempera paintings and ΔE^*_{ab} for the influence of the binder for the same pigment. Following Fig. 8, the atypical behaviour of the egg yolk-based AZ-ST paint resides in the much lower ΔC^*_{ab} compared to the rest of the blue paints. This lower C^*_{ab} variation, neither explained through a mineralogical change of the azurite pigment nor through a chemical modification on the binder, could be explained by the excessive amount of egg added during the pigment preparation by the Kremer manufacturer, which followed the Michel Price method. The objective was to wrap azurite crystals with a proteinaceous compound to protect the pigment against alteration [31].

As reported by Cardell et al. the calculated egg yolk content added to Kremer AZ-ST pigment during the Michel Price procedure was higher (10.5 wt%) than the amount needed for other Kremer azurite pigments made with different grain size (ranging from 2 to 3.5 wt%) [4]. Thus, the higher egg yolk content present in the AZ-ST samples should have a protective effect on the pigment against its deterioration, slowing down its transformation to malachite (normally occurred in azurite tempera), and thus explaining the reduced colour change variation suffered by this sample. Another fact that would support this hypothesis is the greenest colour of the AZ-ST paintings comparatively to the rest of the azurite paint mock-ups. Following the findings of Cardell et al., this green coloration was induced by the high organic content derived from the excess of egg yolk added during the Michel Price method [4].

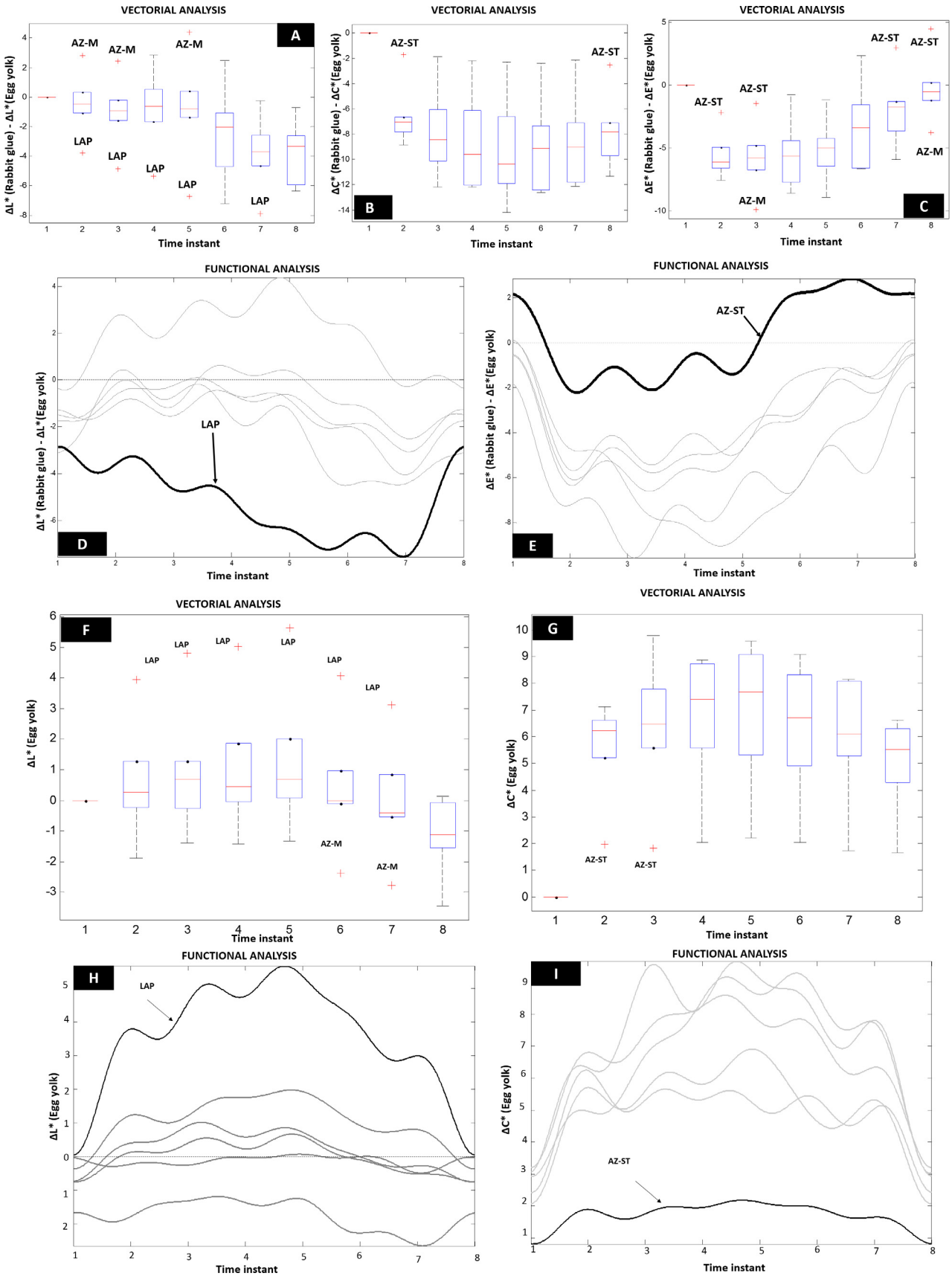

Fig. 7. A–C: Vectorial (box plots) analysis for variable difference between rabbit glue and egg yolk blue tempera data. A: Variable = ΔL^*; B: Variable = ΔC^*_{ab}; C: Variable = ΔE^*_{ab}. D: Functional analysis for ΔL^* differences between rabbit glue and egg yolk blue tempera data. E: Functional analysis for ΔE^*_{ab} differences between rabbit glue and egg yolk blue tempera data. F: Vectorial (box plots) analysis for ΔL^*differences for egg yolk blue tempera data. G: Vectorial (box plots) analysis for ΔE^*_{ab} egg yolk blue tempera data. H: Functional analysis for ΔL^* differences for egg yolk blue tempera data. I: Functional analysis for ΔC^*_{ab} differences for egg yolk blue tempera data.

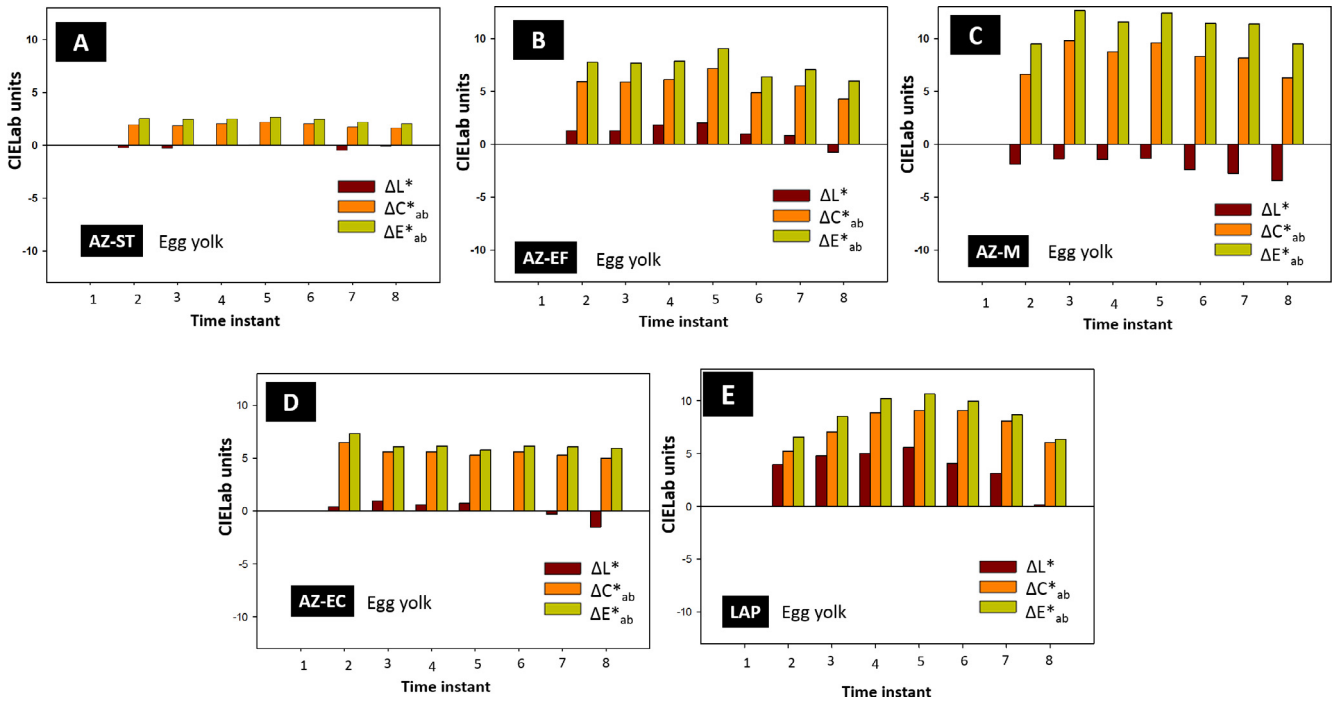

Fig. 8. Colorimetric differences ΔL^*, ΔC^*_{ab}, ΔE^*_{ab}, overtime for some egg yolk blue tempera. A: egg yolk-based AZ-ST paint; B: egg yolk-based AZ-EF paint; C: egg yolk-based AZ-M paint; D: egg yolk-based AZ-EC paint; E: egg yolk-based LAP paint.

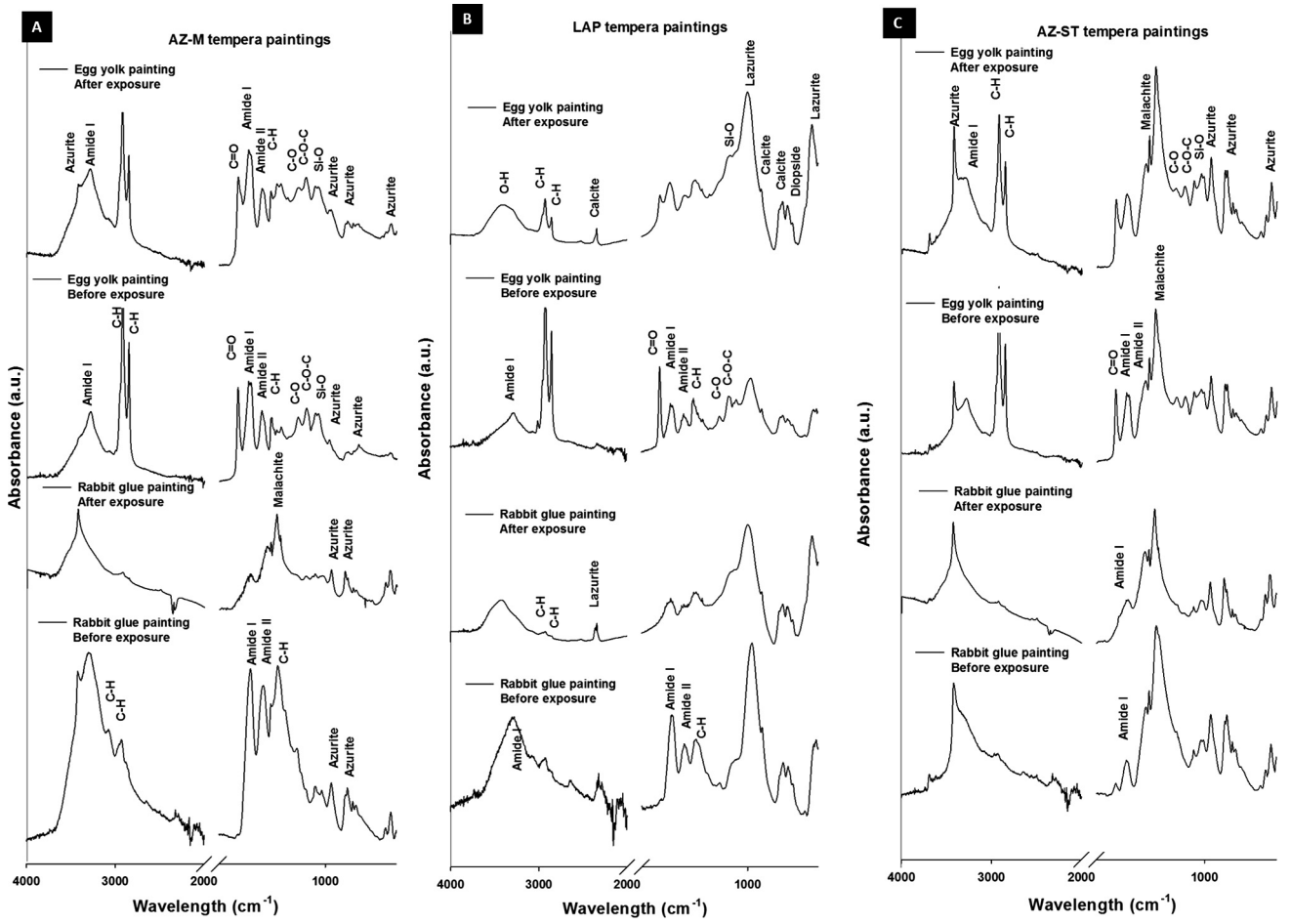

Fig. 9. FTIR (absorbance) spectra of some blue paint mock-ups with either rabbit glue or egg yolk before (initial) and after (final) exposure to outdoor environment. A: AZ-M paintings showing the general trend for the azurite paint mock-ups. B: LAP tempera paintings. C: AZ-ST tempera paintings.

4. Conclusions

In this article two different statistical analyses, i.e. a vectorial (classic) approach and a functional approach, were applied to white, red and blue tempera paint mock-ups outdoor exposed to a marine and industrial environment during thirteen months, to detect different trends on their colour changes. By means of these statistical approaches, the influence of the nature and grain size of the historical pigments, and the nature of the binder (egg yolk and rabbit glue) was analysed.

Both statistic approaches gave similar information concerning the trend of ΔL^*, ΔC^*_{ab} and ΔE^*_{ab} for each colour tempera paint group, and within each colour group, the colour evolution considering the nature of the binder. Although vectorial analysis allowed detecting outliers from the general trend of the data, functional approach has the advantage of refining such identification, avoiding false assignments of atypical behaviours.

Four tempera paint mock-ups showed a statistically significant atypical behaviour. These were: (i) the rabbit glue-based G-M (gypsum medium grained size) paint among the white paint samples, (ii) the egg yolk-based HE (haematite) paint, among the red paint samples, and, (iii) the egg yolk-based AZ-ST (azurite standard grain size) paint and the egg yolk-based LAP (lapis lazuli) paint, among the blue paint mock-ups. It is ruled out that these atypical behaviours are due to mineralogical changes of the pigments happened during the outdoor exposure test. In the egg yolk-based HE and LAP paints, the degradation of the binder during the exposure test, evidenced by the FTIR analysis, seem to be the cause of the different colour change evolution, since on the other tempera samples, the egg yolk binder remained unaltered. Instead, in these two cases, the egg yolk degradation during the outdoor test led to an increase of L^* higher than that suffered by the rest of the tempera mock-ups belonging to their corresponding colour groups.

Conversely, the atypical behaviour of the egg yolk-based AZ-ST paint, characterized by a C^*_{ab} variation lower than the other blue tempera paints, has been related to the high egg yolk content of the AZ-ST tempera mock-up, which make it the greenest of all the azurite-based paints. This unexpected binder content is the sum of the egg yolk added to the AZ-ST pigment by the Kremer manufacturer (following the Michel Price method), in addition to the egg yolk binder mixed to the pigment to prepare the paint mock-up.

All in all, this work has revealed: (i) the need to apply robust statistical techniques allowing the identification of statistically significant atypical behaviours, being the functional approach the most appropriate in time series as correspond to the test performed in this paper, and, (ii) pigment-binder interaction is a key variable in the response of tempera paints to exposure conditions, so that further studies should deepen the knowledge of such interactions by applying alternative analytical techniques and methods.

Acknowledgement

Financial support was provided by the European Regional Development Fund-Belgium (ERDF), Andalusian Research Group RNM-179 and Spanish Research Projects EXPOAIR (P12-FQM-1889) and AERIMPACT (CGL2012-30729).

References

[1] R. Mayer, Materiales y técnicas del arte. Ed. Hermann Blume, Madrid, 1985, 687pp.
[2] E. Manzano, J. Romero-Pastor, N. Navas, L.R. Rodriguez-Simón, C. Cardell, A study of the interaction between rabbit glue binder and blue copper pigment under UV radiation: a spectroscopic and PCA approach, Vib. Spectrosc. 53 (2010) 260–268.
[3] U. Casellato, P.A. Vigato, U. Russo, M. Matteini, Mössbauer approach to the physico-chemical characterization of iron-containings pigments for historical wall paintings, J. Cultural Heritage 1 (2000) 217–232.
[4] C. Cardell, A. Herrera, I. Guerra, N. Navas, L. Rodríguez Simón, K. Elert, Pigment-size effect on the physico-chemical behavior of azurite-tempera dosimeters upon natural and accelerated photo aging, Dyes Pigm. (2017), http://dx.doi.org/10.1016/j.dyepig.2017.02.001.
[5] F. Vanmeert, G.V. der Snickt, K. Janssens, Plumbonacrite identified by X-ray powder diffraction tomography as a missing link during degradation of red lead in a van gogh painting, Angew. Chem. Int. Ed. 54 (2015) 3607–3610.
[6] K. Eremin, J. Stenger, M.L. Green, Raman spectroscopy of Japanese artists' materials: the tale of Genji by Tosa Mitsunobu, J. Raman. Spectrosc. 37 (2006) 1119–1124.
[7] L. Dei, A. Ahle, P. Baglioni, D. Dini, E. Ferroni, Green degradation products of Azurite in wall paintings: identification and conservation treatment, Stud. Conserv. 43 (1998) 80–88.
[8] R. Mazzeo, S. Prati, M. Quaranta, E. Joseph, E. Kendix, M. Galeotti, Attenuated total reflection micro FTIR characterization of pigment-binder interaction in reconstructed paint flims, Anal. Bioanal. Chem. 392 (2008) 65–76.
[9] C.M. Grossi, P. Brimblecombe, Effect of long term changes in air pollution and climate on the decay and blackening of European stone buildings, in: J. Prikryl, B.J. Smith, (Eds.), Building Stone Decay. From Diagnosis to Conservation, vol. 271. Geological Society of London, Special Publications, 2007, pp. 117–130.
[10] M. Urosevic, A. Yebra-Rodríguez, A. Sebastián-Pardo, C. Cardell, Black soiling of an architectural limestone during two-year term exposure to urban air in the city of Granada (S Spain), Sci. Total Environ. 414 (2012) 564–575.
[11] A.C. Iñigo, S. Vicente-Tavera, V. Rives, MANOVA-biplot statistical analysis of the effect of artificial ageing (freezing/thawing) on the colour of treated granite stones, Color Res. Appl. 29 (2004) 115–120.
[12] C. Grossi, P. Brimblecombe, R.M. Esbert, F.J. Alonso, Color changes in architectural limestones from pollution and cleaning, Color Res. Appl. 32 (2007) 320–331.
[13] J.M. Rivas, J. Matías, C. Taboada, Ordóñez, Functional experiment design for the analysis of colour changes in granite using new L∗ a∗ b∗ functional colour coordinates, J. Comput. Appl. Math. 235 (2011) 4701–4716.
[14] F. Pacheco, El arte de la pintura (Ed.), Cátedra, Madrid, Spain, 1990.
[15] G. Vasari, La vida de los más excelentes arquitectos, pintores y escultores escritas por Giorgio Vasari, pintor aretino, UNAM, México, 1996.
[16] A. Martínez-Cortizas, Zonas agroecológicas de Galicia; zona climática FAO, An Edafol Agrobiol 46 (1987) 521–538.
[17] A. Martínez-Cortizas, A. Pérez, (Eds.), Atlas climático de Galicia. Consellería de Medioambiente, Xunta de Galicia; 1999, pp. 210.
[18] Xunta de Galicia, Accesed in April, 2017. Conselleria de Medioambiente e Ordenación do Territorio. Website: <http://www.meteogalicia.gal>.
[19] T. Rivas, S. Pozo, M. Paz, Sulphur and oxygen isotope analysis to identify sources of sulphur in gypsum-rich black crusts developed on granites, Sci. Total Environ. 482–483 (2014) 137–147.
[20] B. Silva, T. Rivas, E. García-Rodeja, B. Prieto, Distribution of ions of marine origin in Galicia (NWSpain) as a function of distance fromthe sea, Atmos. Environ. 41 (2007) 4396–4407.
[21] CIE S014-4/E:2007, Colorimetry Part 4: CIE 1976 L*a*b* Colour Space, Commission Internationale de l'eclairage, CIE Central Bureau, Vienna, 2007.
[22] J.M. Torres, P.J.G. Nieto, L. Alejano, A.N. Reyes, Detection of outliers in gas emissions from urban areas using functional data analysis, J. Hazard. Mater. 186 (1) (2011) 144–149.
[23] J.O. Ramsay, B.W. Silverman, Functional Data Analysis, 2nd ed., Springer-Verlag, New York, 2005, p. 428, ISBN 978-0-387-22751-1.
[24] Y. Zuo, R. Serfling, General notions of statistical depth function, Ann. Stat. 28 (2000) 461–482.
[25] A. Cuevas, M. Febrero, R. Fraiman, On the use of the bootstrap for estimating functions with functional data, Comput. Stat. Data Anal. 51 (2) (2006) 1063–1074.
[26] Q. Wang, W. Sanad, L.M. Miller, A. Voigt, K. Klingel, R. Kandolf, K. Stangl, G. Baumann, Infrared imaging of compositional changes in inflammatory cardiomyopathy, Vib. Spectrosc. 38 (2005) 217–222.
[27] N. Navas, J. Romero-Pastor, E. Manzano, C. Cardell, Benefits of applying combined diffuse reflectance FTIR spectroscopy and principal component analysis for the study of blue tempera historical painting, Analytica Chimica Acta 630 (2008) 141–149.
[28] D. Pellegrini, C. Duce, I. Bonaduce, S. Biagi, L. Ghezzi, M.P. Colombini, M.R. Tinè, E. Bramanti, Fourier transform infrared spectroscopic study of rabbit glue/inorganic pigments mixtures in fresh and aged reference paint reconstructions, Microchem. J. 124 (2016) 31–35.
[29] S. Felder-Casagrande, M. Odlyha, Development of standard paint films based on artists' materials, J. Therm. Anal. 49 (1997) 1585–1591.
[30] R. Meilunas, J.G. Bentsen, A. Steinberg, Analysis of aged paint binders by FTIR spectroscopy, Stud. Conserv. 35 (1990) 33–51.
[31] M. Price, A renaissance of color: particle separation and preparation of azurite for use in oil painting, Leonardo 33 (2000) 281–288.